

Timing models for the long-orbital period binary pulsar PSR B1259–63

N. Wex^{1,2,3}, S. Johnston², R. N. Manchester⁴, A. G. Lyne⁵,
B. W. Stappers⁶ & M. Bailes⁷

¹*Max-Planck Society, Research Unit “Theory of Gravitation”, Max-Wien-Pl. 1, D-07743 Jena, Germany*

²*Research Centre for Theoretical Astrophysics, University of Sydney, NSW 2006, Australia*

³*Max-Planck-Institut für Radioastronomie, Auf dem Hügel 69, D-53121 Bonn, Germany*

⁴*Australia Telescope National Facility, CSIRO, PO Box 76, Epping, NSW 2121, Australia*

⁵*University of Manchester, NRAL, Jodrell Bank, Macclesfield, Cheshire SK11 9DL, UK*

⁶*Mount Stromlo and Siding Spring Observatories, ANU, Private Bag, Weston Creek ACT 2611, Australia*

⁷*University of Melbourne, School of Physics, Parkville, Victoria 3052, Australia*

ABSTRACT

The pulsar PSR B1259–63 is in a highly eccentric 3.4-yr orbit with the Be star SS 2883. Timing observations of this pulsar, made over a 7-yr period using the Parkes 64-m radio telescope, cover two periastron passages, in 1990 August and 1994 January. The timing data cannot be fitted by the normal pulsar and Keplerian binary parameters. A timing solution including a (non-precessing) Keplerian orbit and timing noise (represented as a polynomial of fifth order in time) provide a satisfactory fit to the data. However, because the Be star probably has a significant quadrupole moment, we prefer to interpret the data by a combination of timing noise, dominated by a cubic phase term, and $\dot{\omega}$ and \dot{x} terms. We show that the $\dot{\omega}$ and \dot{x} are likely to be a result of a precessing orbit caused by the quadrupole moment of the tilted companion star. We further rule out a number of possible physical effects which could contribute to the timing data of PSR B1259–63 on a measurable level.

Key words:

pulsar timing – timing noise – binary pulsars – classical spin-orbit coupling – pulsars: individual (PSR B1259–63)

1 INTRODUCTION

The pulsar PSR B1259–63 is a member of a unique binary system. Discovered using the Parkes telescope in a survey of the Galactic plane at 1.5 GHz (Johnston et al. 1992a), it was shown by Johnston et al. (1992b) to be in a highly eccentric 3.4-yr orbit with a 10th-magnitude Be star, SS 2883. The pulsar period, P , is relatively short, 47.8 ms, and the measured period derivative, \dot{P} , gives a pulsar characteristic age, $\tau_c = P/(2\dot{P})$, of 3.3×10^5 yr and a surface magnetic field of 3.3×10^{11} G. This therefore is a young system, which may evolve through an accretion phase to form a single or binary millisecond pulsar. Rapidly spinning neutron stars can only accrete matter if the co-rotation velocity at the Alfvén radius is less than the Keplerian velocity at the same radius (Bhattacharya & van den Heuvel 1991). Equality of these velocities defines the ‘spin-up line’. At present, PSR B1259–63 lies well to the left of the spin-up line, so that accretion onto the neutron star is not possible until either the pulsar slows down or the pulsar magnetic field decays.

Timing observations of PSR B1259–63, made over a

3.4-yr interval and covering the 1990 August periastron, were reported by Johnston et al. (1994). A phase-connected fit to these data gave parameters for the pulsar and its orbit, and showed that the next periastron would occur on 1994 January 9. This paper also reported optical observations which indicate that the companion star is of spectral type B2e, with a mass of $m_* \sim 10 M_\odot$ and radius $R_* \sim 6 R_\odot$. The break-up velocity at the equator, v_{\max} , for B2e stars is not very well known; it is estimated to be ~ 380 km s^{-1} by Slettebak et al. (1980) and ~ 480 km s^{-1} by Schmidt-Kaler (1982). Recent work by Porter (1996) suggests that most Be stars rotate at ~ 70 per cent of the break-up velocity. From the mass function, a companion mass of $10 M_\odot$ and a pulsar mass, m_p , of $1.4 M_\odot$ imply an orbital inclination $i = 36^\circ$. The orbital eccentricity is very high, 0.87, and the pulsar approaches within $24 R_*$ of the companion star at periastron, passing through the circumstellar disk. Extensive observations of the pulsar were made at several radio frequencies before and after the 1994 January periastron, in order to probe the circumstellar environment of SS

2883 (Johnston et al. 1996; Melatos, Johnston & Melrose 1995).

Observations made between 1990 January and 1994 October were well explained by step changes in the pulsar period at the two periastrons (Manchester et al. 1995), attributed to a propeller-torque spin-down caused by the interaction of the pulsar with the circumstellar matter at the Alfvén radius (Illarionov & Sunyaev 1975, King & Cominsky 1994, Ghosh 1995).

In this paper we report on additional timing observations made using the Parkes radio telescope over the past two years which, together with the earlier data, give a total timing data span of seven years. We find that the timing solution of Manchester et al. (1995) does not fit the recent data and discuss alternative models and their interpretation.

2 TIMING OBSERVATIONS AND DATA ANALYSIS

A total of ~ 300 pulse times of arrival (TOAs) were measured at the Parkes radio telescope between 1990 January and 1996 December. Most of the observations were at frequencies around 1.5 GHz, but observations at 0.43, 0.66, 4.8 and 8.4 GHz were also made. At all frequencies, dual-channel cryogenically cooled systems receiving orthogonal linear polarizations were used. After conversion to an intermediate frequency, signals for each polarization were split into subbands using filterbanks with channel widths of 0.125 or 0.25 MHz for frequencies below 1 GHz, and 5 MHz for higher frequencies. Signals from corresponding filter polarization pairs were detected, summed, high-pass filtered and one-bit digitized, usually with a sampling interval of 0.6 ms. Further details of the observing systems are given in Johnston et al. (1996).

The data were folded at the topocentric period to form mean pulse profiles. Integration times were typically 10 min at 1.5 GHz, and 20 to 30 min at other frequencies. Data taken prior to 1994 were convolved with a ‘standard profile’ in the time domain to produce TOAs whereas data taken after 1994 were processed using a different method which involves matching the Fourier components of the observed and standard profiles. Uncertainties in the TOAs are somewhat smaller using the second method. However in order not to bias the fitting procedure towards the second half of the data (i.e. the second orbit), we use *unweighted* fits throughout this paper; that is, all TOAs were assigned the same weight regardless of the estimated TOA uncertainty. Also, we use only TOAs obtained at frequencies around 1.5 GHz and those TOAs at 4.8 GHz, which show the best signal-to-noise ratio, in order to obtain a good value for the dispersion measure. Pulsar and binary parameters were obtained using the least-squares fitting program TEMPO (Taylor & Weisberg 1989) with the Jet Propulsion Laboratory solar-system ephemeris DE200 (Standish 1982). TEMPO was extended by the addition of a new timing model for binary pulsars that orbit a companion star with a significant quadrupole moment (Wex 1998).

As discussed by Johnston et al. (1996), significant dispersion and scattering changes were observed around periastron. Because of this, data from 1990 July and 1993 December were omitted from the analysis. The pulsar was eclipsed

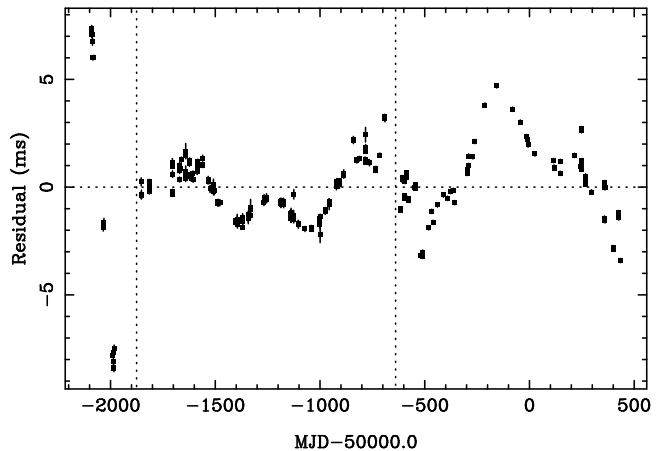


Figure 1. Post-fit residuals from an unweighted fit for pulsar position, period, period derivative, dispersion measure and Keplerian orbital parameters. The rms residual is $2100 \mu\text{s}$. The vertical dotted lines in this and subsequent figures indicate the two epochs of periastron passage.

during 1994 January. Thus, the two largest gaps in the data in terms of true anomaly, φ , are one of 129 days around the first periastron ($\varphi = -145^\circ \dots 100^\circ$) and 76 days around the second periastron ($\varphi = -128^\circ \dots 105^\circ$). This will emerge to be a problem when searching for the correct timing model for PSR B1259–63.

The data were first fitted for pulsar position, period, period derivative, dispersion measure, and the five Keplerian orbital parameters. The best results give an rms residual of $2100 \mu\text{s}$ and the post-fit residuals shown in Fig. 1. Systematic variations in the residuals are observed at all orbital phases, showing that this set of parameters does not model the timing behaviour of the system satisfactorily.

Three types of model are considered in the following subsections with a view to minimising these residuals and understand their origin.

2.1 Period steps at periastron

As mentioned in the Introduction, observations made between 1990 January and 1994 October were well fitted by step increases in the pulsar period at the two periastrons. Fig. 2 shows the pre-fit residuals obtained using the timing solution given in Manchester et al. (1995) on the extended data set. Clearly, the timing observations made in 1995 and 1996 are not modelled by this solution.

There is other evidence which suggests that propeller spin-down does not occur at periastron. Models of the system by Tavani & Arons (1997) based on extensive X-ray and γ -ray observations during the 1994 periastron (Kaspi et al. 1995, Hirayama et al. 1996, Grove et al. 1995) conclude that accretion or propeller-powered processes are ruled out.

If we allow fitting for a period step at the two periastrons, we find a rather good fit, with rms residual of $340 \mu\text{s}$. However, the two period steps have opposite sign, $\Delta\nu = -1.7 \times 10^{-8}$ at the first periastron and $\Delta\nu = 2.6 \times 10^{-8}$ at the second periastron. This does not seem physically plausible and this evidence, coupled with the X-ray studies, causes us to rule out this physical mechanism as an explanation for the timing residuals in PSR B1259–63.

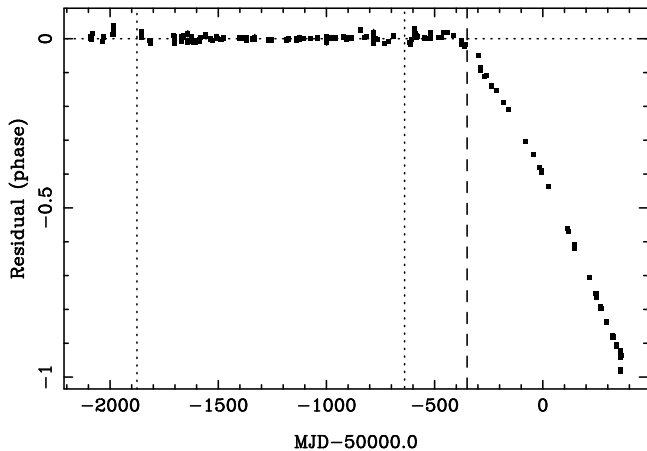


Figure 2. Pre-fit residuals for the Manchester et al. (1995) timing solution. The vertical dashed line indicates the end of the Manchester et al. (1995) data set.

2.2 Timing noise

PSR B1259–63 is a comparatively young pulsar with a period derivative, \dot{P} , of 2.3×10^{-15} . Such a young pulsar should suffer timing noise which is usually dominated by a cubic term and may contain higher-order derivatives (Lyne 1996). For a pulsar with such a period first derivative the expected value of \ddot{P} is of order $\pm 2 \times 10^{-26} \text{ s}^{-1}$. (The intrinsic \ddot{P} arising from magnetic dipole spin-down, i.e. assuming a braking index of 3, is expected to be only of order 10^{-28} s^{-1} .) Fitting for \ddot{P} , \dddot{P} and \ddot{P} terms gives the residuals illustrated in Fig. 3 and an rms residual of only $350 \mu\text{s}$. Parameters for this fit are given in Table 1 as Model 1. The value for \ddot{P} is within the expected range. Fitting for a \ddot{P} does not improve the fit and does not give significant values for this parameter.

The parameters in this fit are uncertain in the sense that they are relatively insensitive to adding or subtracting an integral number of phase turns at the two periastrons, provided that the number of turns added or subtracted was the same at each periastron. This ambiguity arises because of the large (~ 100 days) gap in the data resulting from the pulsar eclipse at each periastron. Quoted parameter-error estimates take this uncertainty into account by reflecting the parameter range for added or subtracted turns giving satisfactory solutions, that is, increasing the rms residual by less than 20 per cent. Up to 3 phase turns could be added or subtracted at each periastron within this criterion.

It is difficult to derive an ‘activity parameter’ (Cordes & Helfand 1980) for binary pulsars, especially for long-period binaries where some of the timing noise may be taken up in the orbital parameters. Having removed the lower order terms in the fitting process above, the remaining residuals in Fig. 3 are probably the higher order terms of the noise process. In particular, the timing residuals are very similar to those of PSR B1951+32 (Foster et al. 1994), a solitary pulsar of similar period and youth to PSR B1259–63.

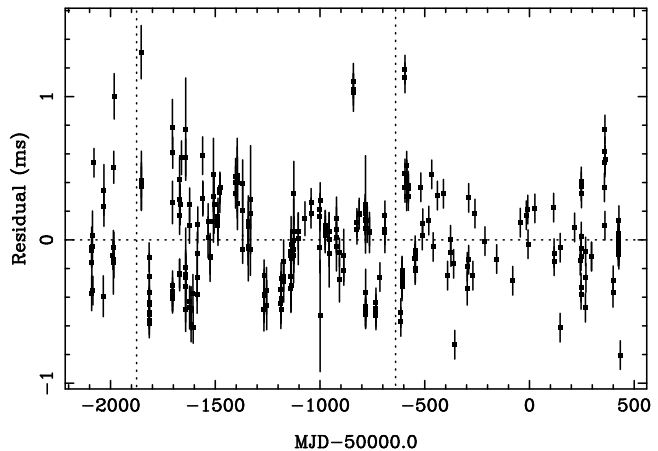


Figure 3. Post-fit residuals for Model 1, i.e. fitting for pulsar position, period, period derivative, dispersion measure, Keplerian orbital parameters, and \ddot{P} , \dddot{P} and \ddot{P} to model the timing noise. The rms residual is $350 \mu\text{s}$.

2.3 Secular changes in the orbit ($\dot{\omega}$, \dot{x}) and classical spin-orbit coupling

For a pulsar in orbit with a Be star, one may expect changes in the longitude of the periastron, ω , and the inclination of the orbit, i , (Lai et al. 1995). The latter manifests itself as a change of the projected semi-major axis $x = a_p \sin i$. The physical cause of these changes is the ‘classical spin-orbit coupling’, i.e. the fact that the spin-induced quadrupole of the fast-rotating companion leads to a $1/r^3$ term in the gravitational potential which in turn leads to apsidal motion and precession of the binary orbit (Kopal 1978, Smarr & Blandford 1976, Lai et al. 1995, Wex 1998).

Two unweighted fits for the pulsar-spin parameters, including a \ddot{P} to model the long-term behaviour of the timing noise, the Keplerian parameters for orbital motion, and the two post-Keplerian parameters, $\dot{\omega}$ and \dot{x} , are given in Table 1 (Model 2A and Model 2B). The corresponding post-fit residuals are shown in Fig. 4. Again, realistic errors for the parameters in the table were obtained by adding (or subtracting) an integer number of phase turns at each periastron until the fit deviated from the best fit by about 20 per cent. In this case, however, two satisfactory independent fits could be obtained by having, in the case of Model 2A, an equal number of phase turns at the two periastrons and, in the case of Model 2B, one more phase turn at the second periastron.

Let us assume that all the timing noise is modelled by \ddot{P} , i.e. that the fitted $\dot{\omega}$ and \dot{x} result only from changes in the orientation of the binary orbit due to classical spin-orbit coupling, and focus on the question: can the values for $\dot{\omega}$ and \dot{x} , as given in Table 1, be explained by a reasonable quadrupole moment and orientation of the Be star?

In the case of PSR B1259–63, the spin angular momentum of the pulsar is completely negligible compared to the spin angular momentum \mathbf{S} of the companion and the (total) orbital angular momentum \mathbf{L} . The angle θ_J between the conserved total angular momentum $\mathbf{J} = \mathbf{L} + \mathbf{S}$ and \mathbf{L} is also conserved (see Fig. 5). The intersection of the orbital plane (perpendicular to \mathbf{L}) and the invariable plane (perpendicular to \mathbf{J}) has the longitude Φ and the longitude of the

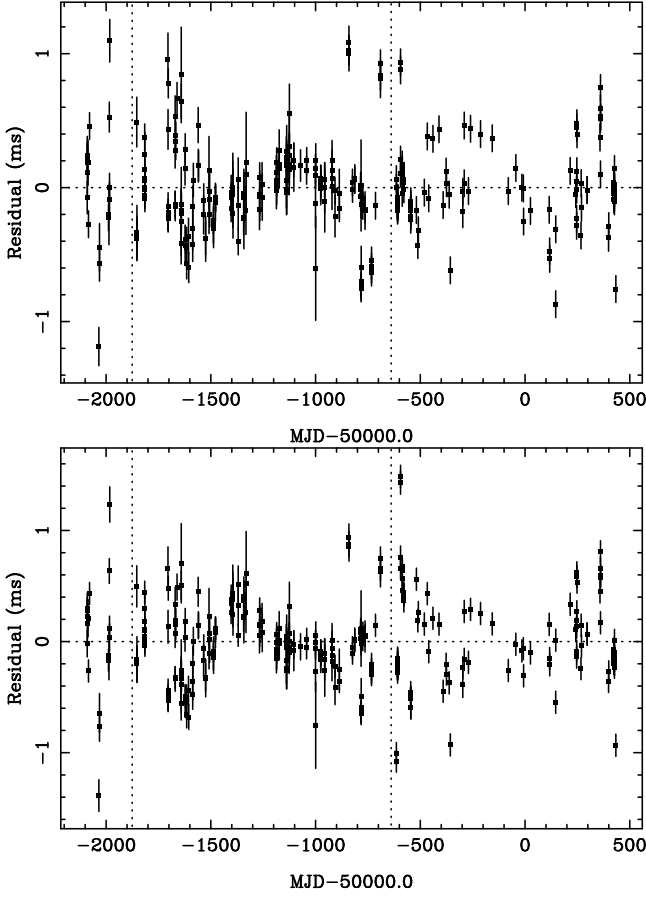


Figure 4. Post-fit residuals for Model 2A (upper) and Model 2B (lower), i.e. fitting for pulsar position, period, period derivative, dispersion measure, Keplerian orbital parameters, $\dot{\omega}$, \dot{x} and \dot{P} to model the timing noise, using the BT++ timing model (see Wex 1998). The two models differ in the number of turns added at periastron (see text). Model 2A has an rms residual of $340 \mu\text{s}$ and Model 2B an rms residual of $390 \mu\text{s}$.

periastron with respect to the invariable plane is denoted by Ψ . The angle between \mathbf{L} and the direction of sight \mathbf{K}_0 is denoted by i . The angle i is not uniquely determined by timing observations and is equal to either 36° or $180^\circ - 36^\circ$ for PSR B1259–63.

The classical spin-orbit coupling causes a (linear-in-time) precession of the angles Φ and Ψ which implies a rather complicated change of the angles i and ω . For the case $|\mathbf{S}| \ll |\mathbf{L}|$ [†] the changes of the longitude of periastron, ω , and the projected semi-major axis, x , are approximated by

$$\dot{\omega}_Q \simeq \frac{3n^{7/3} \tilde{J}_2^*}{2(GM)^{2/3}(1-e^2)^2} \times \left(1 - \frac{3}{2} \sin^2 \theta + \cot i \sin \theta \cos \theta \cos \Phi \right), \quad (1)$$

$$\frac{\dot{x}_Q}{x} \simeq \frac{3n^{7/3} \tilde{J}_2^*}{2(GM)^{2/3}(1-e^2)^2} \cot i \sin \theta \cos \theta \sin \Phi, \quad (2)$$

[†] For PSR B1259–63, $|\mathbf{S}| \sim 0.1|\mathbf{L}|$. The approximation $|\mathbf{S}| \ll |\mathbf{L}|$ is justified for the accuracy required here.

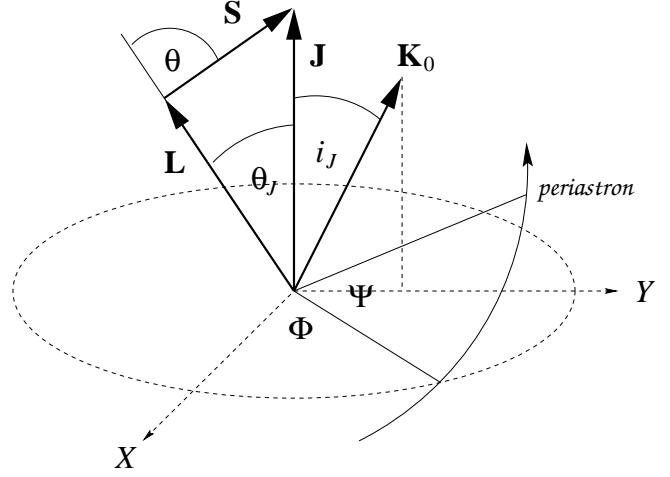


Figure 5. Definition of different angles in the binary system. The invariable plane (X - Y) is perpendicular to the total angular momentum $\mathbf{J} = \mathbf{L} + \mathbf{S}$, and the line-of-sight unit vector \mathbf{K}_0 lies in the Y - Z plane. θ_J is the inclination of the orbital plane with respect to the invariable plane, Φ is the longitude of the ascending node with respect to the invariable plane and Ψ is the longitude of the periastron with respect to the invariable plane. θ is the inclination of the companion spin with respect to the orbital angular momentum. i_J and i are the angles between the line of sight and \mathbf{J} and \mathbf{L} respectively.

(Smarr & Blandford 1976, Lai et al. 1995, Wex 1998). $n \equiv 2\pi/P_b$ is the orbital frequency of the binary system, G is the gravitational constant, and $M = m_p + m_*$ the total mass of the system. The quantity \tilde{J}_2^* is a measure of the quadrupole moment of the Be star

$$\tilde{J}_2^* \equiv \frac{I_3^* - I_1^*}{m_*} = \frac{2}{3} k R_*^2 \hat{\Omega}_*^2, \quad (3)$$

where $\hat{\Omega}_* \equiv \Omega_*/(Gm_*/R_*^3)^{1/2}$ is equal to unity if the star is rotating near break-up. I_3^* and I_1^* are the moments of inertia about the spin axis and an orthogonal axis, respectively. R_* is the (equatorial) radius of the Be star and k is the apsidal motion constant which is of the order of 0.01 for a $10 M_\odot$ main-sequence star (Schwarzschild 1958; Claret & Gimenez 1992). Assuming a typical radius of $R_* \approx 6R_\odot$ and a rotation of $\hat{\Omega}_* \approx 0.7$ for the Be-star companion we find

$$\tilde{J}_2^* \sim 0.1 R_\odot^2 = 2.2 \times 10^{-6} \text{ AU}^2. \quad (4)$$

The ratio of equations (1) and (2) leads to

$$\frac{\dot{\omega}_Q x}{\dot{x}_Q} \sin \Phi - \cos \Phi = \frac{1 + 3 \cos 2\theta}{2 \cot i \sin 2\theta}, \quad (5)$$

an equation that does not contain the uncertain quantity \tilde{J}_2^* .

The observed value of $\dot{\omega}$ (see Table 1) is a compound of $\dot{\omega}_Q$ and the general relativistic contribution

$$\dot{\omega}_{GR} \approx +0.00003 \text{ deg yr}^{-1}. \quad (6)$$

Thus we have for PSR B1259–63

$$\text{MODEL 2A : } \begin{cases} \dot{\omega}_Q = -0.00021(1) \text{ deg yr}^{-1} \\ \dot{x}_Q = -0.15(3) \times 10^{-10} \end{cases} \quad (7)$$

$$\text{MODEL 2B : } \begin{cases} \dot{\omega}_Q = -0.00043(1) \text{ deg yr}^{-1} \\ \dot{x}_Q = -2.40(4) \times 10^{-10} \end{cases} \quad (8)$$

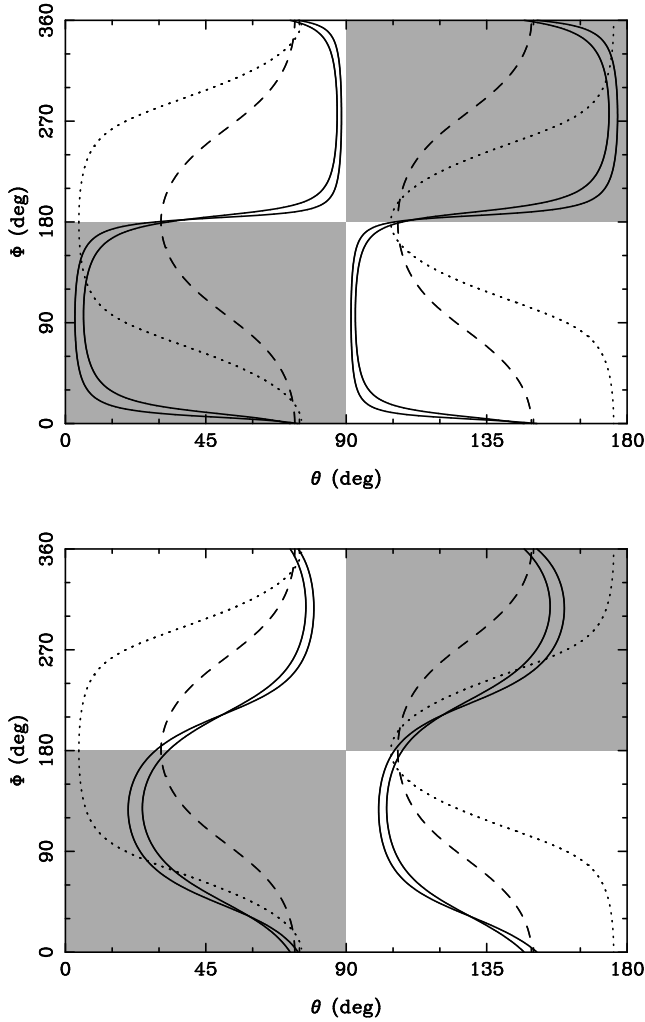


Figure 6. θ - Φ parameter space for Model 2A (upper) and Model 2B (lower) for the case $i = 36^\circ \pm 5^\circ$. (for $i = 144^\circ \pm 5^\circ$ one has to replace Φ by $\Phi - 180^\circ$). The grey areas are excluded because $\dot{\Phi} < 0$. The regions to the left of the left dashed curve and to the right of the right dashed curve are excluded because $\dot{\omega}_0 < 0$. The solid curves border the narrow region of possible values of θ and Φ . For the regions to the left of the left dotted curve and to the right of the right dotted curve the Be star’s rotation exceeds 70% of the break-up velocity.

The restrictions implied by equation (5) are plotted in Fig. 6 which, in addition, shows restrictions implied by optical observations of the projected stellar rotation velocity, v_{obs} :

$$\pm \sqrt{1 - \left(\frac{v_{\text{obs}}}{\hat{\Omega}_* v_{\text{max}}} \right)^2} = \cos i \cos \theta + \sin i \sin \theta \cos \Phi, \quad (9)$$

where v_{max} is the break-up velocity. For SS 2883 one finds 180 km s^{-1} for v_{obs} (Johnston et al. 1994). As mentioned in Section 1, the break-up velocity for Be stars is not very well known; we use $v_{\text{max}} = 400 \text{ km/s}$ as the break-up velocity of SS 2883. If we assume that SS 2883 rotates at 70% of its break-up velocity ($\hat{\Omega}_* = 0.7$) we get the dotted line in Fig. 6 and allowed values of (θ, Φ) are therefore close to $(75^\circ, 355^\circ)$ and $(105^\circ, 175^\circ)$.

The large value of θ implies a significant birth kick to the neutron star (cf. Kaspi et al. 1996). Since recent mea-

surements of pulsar velocities suggest kicks of $200 - 400 \text{ km s}^{-1}$ are commonplace (Lyne & Lorimer 1994), there is a high probability that PSR B1259–63 was kicked into a highly inclined orbit; indeed, there is a high probability that an eccentric orbit resulting from a birth kick is retrograde (Hills 1983).

Using equations (1) and (5) one can calculate \ddot{J}_2^* as a function of Φ , and so using equation (3) one obtains kR_*^2 as a function of Φ . Assuming that $R_* \approx 6R_\odot$ for B2e stars, we find those values for the apsidal motion constant k which are necessary to explain the parameters $\dot{\omega}$ and \dot{x} for Models 2A and 2B by classical spin-orbit coupling exclusively. We find that Models 2A and 2B need rather large values for the apsidal motion constant k . While the minimum value for Model 2A, $k = 0.02$, is still in the range of theoretical models (Claret & Giménez 1991), the value of $k = 0.05$, necessary for Model 2B, seems to be too large.

As in the previous section, this model provides a good explanation of the data, i.e. this solution maintains phase to better than 3% of the rotational period. The remaining residuals are fully consistent with higher order terms of the timing noise (c.f. end of Section 2.2). However, it is likely in this case that such timing noise cannot fully be removed with a \ddot{P} term and that this may affect the measured values of $\dot{\omega}$ and \dot{x} and hence the derived values for θ and Φ . This introduces an additional uncertainty which is not represented by the quoted error limits.

Simulations suggest that observations around and after the next periastron (1997 May 29) should distinguish between the various models.

3 FURTHER EFFECTS ON THE ORBITAL MOTION

Besides quadrupolar effects resulting from the oblateness of the Be star, orbital perturbations could arise from tidal effects on the Be star, frictional drag as the pulsar passes through the circumstellar disk, and mass loss from the Be star. We will show that the major influence of these effects is to change the orbital period, P_b , by at most 3 seconds per orbital period ($\dot{P}_b \lesssim 3 \times 10^{-8}$). However if we additionally fit for \dot{P}_b in the models described above, the rms does not change (i.e. the value of \dot{P}_b is not significant) and the 1σ errors on \dot{P}_b are of order 10^{-5} . Hence none of these effects have any impact on the current timing solution at a measurable level.

3.1 Tidal effects

In the case of PSR B1259–63, perturbations due to tidal effects were investigated by several authors using standard theory of tidal dissipation and found to be negligible (Kochanek 1993, Manchester et al. 1995, Lai et al. 1995).

Recent work by Lai (1996,1997) and Kumar & Quataert (1997) shows that (differential) stellar rotation can change the strength of the dynamical tide significantly. In particular, retrograde rotation (with respect to the orbital motion of the pulsar) increases the energy and angular-momentum transfer by more than two orders of magnitude. This effect is most likely the explanation for the observed \dot{P}_b of 3×10^{-7} in the main-sequence star binary pulsar PSR J0045–7319

(Kaspi et al. 1996). However the periastron distance of PSR J0045–7319 from its companion is only 4 stellar radii, while PSR B1259–63 passes periastron at a distance of 24 stellar radii and thus the strength of the dynamical tides is several orders of magnitude smaller. Following calculations in Lai (1996) we find for PSR B1259–63

$$\dot{P}_b \sim -10^{-10} \left(\frac{50 \text{ yr}}{\tau_d} \right) \left(\frac{T_2(\eta)}{0.001} \right), \quad (10)$$

where τ_d is the dissipation time for the dynamical tide and $\eta = (m_*/M)^{1/2}(r_{\text{peri}}/R_*)^{3/2}$ where r_{peri} is the periastron distance. The function $T_2(\eta)$ depends strongly on the rotation rate of the companion star and increases with decreasing values for $\hat{\Omega}_*$. Assuming nearly maximum retrograde rotation of the companion star, Lai (1997) found $T_2 = 0.01$ for PSR J0045–7319 ($\eta = 7$). For PSR B1259–63, T_2 should be clearly smaller, since $\eta = 110$ for this binary system; one expects $T_2 \lesssim 0.001$. Therefore, for realistic values of the dissipation time, τ_d , the dynamical tides are absolutely negligible in the PSR B1259–63 system.

3.2 Frictional drag

A fit to dispersion-measure changes around the 1994 January periastron (Johnston et al. 1996) indicates that the radial dependence of the electron density in the circumstellar disk of SS 2883 has the form

$$n_e(r) \sim 4.5 \times 10^{12} (r/R_*)^{-4.2} \text{ cm}^{-3}. \quad (11)$$

Assuming a hydrogen plasma, this corresponds to a mass density

$$\rho_H(r) \sim 7.5 \times 10^{-12} (r/R_*)^{-4.2} \text{ g cm}^{-3}. \quad (12)$$

The radius within which matter is captured by the pulsar is given by the Bondi (1952) relation

$$r_{\text{acc}} = \frac{2Gm_p}{v_{\text{rel}}^2} \approx \frac{3.7 \times 10^{12} \text{ cm}}{(v_{\text{rel}}/100 \text{ km s}^{-1})^2}, \quad (13)$$

where v_{rel} is the velocity relative to the surrounding medium. The drag acceleration induced by the accretion of matter onto the neutron star is then given by

$$\mathbf{A} = -\frac{\pi r_{\text{acc}}^2 \rho_H v_{\text{rel}} \mathbf{v}_{\text{rel}}}{m_p}. \quad (14)$$

To estimate if friction has an important effect on the orbital motion of PSR B1259–63, we assume that the circumstellar disk is not inclined with respect to the orbital plane, implying a maximum effect. We further assume (to simplify the calculations) that the velocity of the pulsar around periastron ($\sim 150 \text{ km s}^{-1}$) is much larger than the velocity of the circumstellar material[‡]. In this case the direction of the friction is roughly anti-parallel to the velocity of the pulsar, $\mathbf{v}_{\text{rel}} = \mathbf{v}_p$. Friction will not affect the plane of the orbit, but it will affect the Keplerian parameters. For the change of the orbital period P_b , eccentricity e , and longitude of periastron ω one finds (see e.g. Danby 1962)

[‡] The velocity of the circumstellar matter is expected to be of the order of 150 to 300 km s^{-1} (Waters 1986; Bjorkman & Cassinelli 1993). Although we neglect this fact, we will still obtain the correct order of magnitude.

$$\dot{P}_b = \frac{3P_b^{4/3} v}{(2\pi GM)^{2/3}} A, \quad (15)$$

$$\dot{\omega} = \frac{2 \sin \varphi}{ev} A, \quad (16)$$

$$\dot{e} = 2 \frac{\cos \varphi + e}{v} A, \quad (17)$$

where φ is the true anomaly of the pulsar and v the absolute value of the relative velocity between the pulsar and its companion. Integration of these equations leads to the following change of the orbital parameters during one orbital revolution:

$$\Delta P_b \approx -0.002 \text{ s}, \quad (18)$$

$$\Delta \omega = 0, \quad (19)$$

$$\Delta e \approx -3 \times 10^{-13}. \quad (20)$$

These values are well below the present measurement precision. Thus we conclude, in agreement with Manchester et al. (1995), that frictional drag has a negligible effect on the TOAs of PSR B1259–63.

From equation (20), we can calculate the typical time scale for circularisation:

$$\tau_{\text{circ}} \gtrsim \frac{e}{\Delta e} P_b \sim 10^{13} \text{ yr}. \quad (21)$$

There are indications that the circumstellar disk is tilted with respect to the orbital plane (Johnston et al. 1996). Therefore the pulsar is within the circumstellar disk twice per orbit, but only for a comparatively short time, which reduces the effect of friction by at least an order of magnitude. Furthermore there is no evidence that any accretion of material onto the pulsar took place during the 1994 periastron passage (Tavani & Arons 1997).

3.3 Mass loss of the companion

If the companion star loses mass at a rate \dot{m}_* so that there is no linear momentum loss in the instantaneous rest frame of the star, the orbital period will change by a rate given by (Jeans 1924, 1925)

$$\frac{\dot{P}_b}{P_b} = -\frac{2\dot{m}_*}{m_* + m_p}. \quad (22)$$

The mass loss of SS 2883 is of order $-5 \times 10^{-8} M_\odot \text{ yr}^{-1}$ (Johnston et al. 1996) and so

$$\dot{P}_b \sim 3 \times 10^{-8}, \quad (23)$$

which gives an orbital period change of ~ 3 seconds per orbital revolution, a value which is well below measurement precision.

4 RELATIVISTIC EFFECTS

Because of the high eccentricity and the large mass of the companion there are two relativistic effects which should be considered: the Einstein delay described by the post-Keplerian parameter γ (Blandford & Teukolsky 1976), and the Shapiro delay, which depends on the orbital inclination i of the binary system and is proportional to the mass of the companion (Damour & Deruelle 1986).

For PSR B1259–63, the parameter γ is quite large. We find

$$\gamma = \frac{1}{c^2} \left(\frac{P_b}{2\pi} \right)^{1/3} \frac{G^{2/3} m_* (m_p + 2m_*)}{(m_p + m_*)^{4/3}} e \simeq 0.54 \text{ s}. \quad (24)$$

As pointed out by Blandford & Teukolsky (1975) and Brumberg et al. (1975), γ can be isolated only in the presence of apsidal motion and requires observations over a time interval in which ω changes by a significant amount. Since, for PSR B1259–63, ω changes by a few arcseconds each orbital revolution and less than two orbital revolutions have been observed, we cannot extract γ from the present data; it is absorbed into the Keplerian parameters x and ω . To a first approximation we find

$$x \rightarrow x + \frac{\gamma \cos \omega}{(1 - e^2)^{1/2}} \simeq x - 0.84 \text{ sec}, \quad (25)$$

$$\omega \rightarrow \omega - \frac{\gamma \sin \omega}{x(1 - e^2)^{1/2}} \simeq \omega - 0^\circ 031. \quad (26)$$

Thus the observed values are offset from the true values by a few hundred times the errors of the measurements.

A second potentially important relativistic effect is the Shapiro delay, the propagation delay caused by the gravitational potential of the companion star. The delay is given by (Damour & Deruelle 1986)

$$\Delta_S = -\frac{2Gm_*}{c^3} \ln \left\{ 1 - e \cos U - [\sin \omega (\cos U - e) + (1 - e^2)^{1/2} \cos \omega \sin U] \sin i \right\}, \quad (27)$$

where U is the eccentric anomaly of the binary orbit. For PSR B1259–63 ($i \approx 35^\circ$) Δ_S has a range of 400 μs and thus is much greater than the error in most of the TOAs. The fact that there are no observations around periastron where there is a sharp peak in Δ_S reduces the actual span of Δ_S to 150 μs . This remaining effect can be absorbed in the other parameters without changing them by more than the typical given error (see Table 1).

5 CONCLUSIONS

At present, the timing observations for the binary pulsar PSR B1259–63 span seven years. Because of the gaps in timing observations around the two periastrons and the large timing noise present in this young pulsar, we still are not able to derive a unique timing model to explain the TOAs.

Model 1 is a timing solution including a non-precessing Keplerian orbit and timing noise represented as a polynomial of fifth order in time. This model provides a satisfactory fit to the data. The remaining timing residuals are understood as short-term timing noise similar to that seen in observations of other young pulsars (cf. Foster et al. 1994).

Equally good results were obtained by Model 2 and 3. Both timing models contain just a \ddot{P} term to account for the long-term behaviour of the timing noise, and $\dot{\omega}$ and \dot{x} , which both are understood to result from a precession of the orbit. This orbital precession can be explained by the classical spin-orbit coupling caused by the quadrupolar nature of the main-sequence star companion. The corresponding advance of periastron is negative and thus the companion should be tilted by more than 30° with respect to the orbital plane (See Fig. 6). This can be explained by a birth kick for the pulsar (cf. Kaspi et al. 1996).

Tidal dissipation and frictional drag in the circumstellar matter is shown to be negligible. The influence of the mass loss of the companion is too small to be detectable unless the mass loss is $\gtrsim 10^{-5} M_\odot/\text{yr}$. At the same time we can exclude a significant orbital period change in the TOAs of PSR B1259–63.

PSR B1259–63 should show the largest Einstein delay and largest Shapiro delay of all known binary pulsars. The small change in the longitude of periastron makes it impossible to isolate the Einstein delay. The Shapiro delay peaks sharply around periastron and is so far unobservable.

Again, we stress that the physical parameters given here for the companion star, θ , Φ and k , should be understood as one possible explanation for the significant values of $\dot{\omega}$ and \dot{x} in Models 2A and 2B. If the long-term behaviour of the timing noise of PSR B1259–63 is not fully modelled by a cubic term (\ddot{P}), it is possible that rather large fractions of these parameters are not explained by a precession of the orbital plane but have their origin in unmodelled timing noise. The parameters here show that, in principle, all of the $\dot{\omega}$ and \dot{x} can arise from classical spin-orbit coupling, for Model 2A in particular.

Although Model 1 gives a good fit to the TOAs without making use of the classical spin-orbit coupling, it seems unlikely that the classical spin-orbit coupling is of no importance for this system.

ACKNOWLEDGMENTS

We thank the Parkes staff for their assistance, N. D’Amico, B. Koribalski and L. Nicastro for help with these observations and J. H. Taylor for useful comments. The Australia Telescope is funded by the Commonwealth of Australia for operation as a National Facility managed by the CSIRO.

REFERENCES

- Barker B. M., O’Connell R. F., 1975, Phys. Rev. D, 12, 329
 Bhattacharya D., van den Heuvel E. P. J., 1991, Phys. Rep., 203, 1
 Bjorkman J. E., Cassinelli J. P., 1993, ApJ, 409, 429
 Blandford R., Teukolsky, S. A., 1975, ApJ, 198, L27
 Blandford R., Teukolsky, S. A., 1976, ApJ, 205, 580
 Bondi H., 1952, MNRAS, 112, 195
 Brumberg V. A., Zel’dovich Y. B., Novikov I. D., Shakura N. I., 1975, Astr. Lett., 1, 5
 Claret A., Gimenez A., 1992, A&AS, 96, 255
 Cordes J. M., Helfand D. J., 1980, ApJ, 239, 640
 Damour T., Deruelle N., 1985, Ann. Inst. Henri Poincaré, 43, 107
 Damour T., Deruelle N., 1986, Ann. Inst. Henri Poincaré, 44, 263
 Damour T., Taylor J. H., 1992, Phys. Rev. D, 45, 1840
 Danby J. M. A., 1962, Fundamentals of Celestial Mechanics, The MacMillan Company, New York
 Foster R. S., Lyne A. G., Shemar S. L., Backer D. C., 1994, AJ, 108, 175
 Ghosh P., 1995, ApJ, 453, 411
 Hills J. G., 1983, ApJ, 267, 322
 Hirayama M., Nagase F., Tavani M., Kaspi V. M., Kawai N., Arons J., 1996, PASJ, 48, 833
 Illarionov A. F., Sunyaev R. A., 1975, A&A, 39, 185
 Jeans J. H., 1924, MNRAS, 84, 2
 Jeans J. H., 1925, MNRAS, 85, 912

- Johnston S., Lyne A. G., Manchester R. N., Kniffen D. A., D'Amico N., Lim J., Ashworth M., 1992a, MNRAS, 255, 401
- Johnston S., Manchester R. N., Lyne A. G., Bailes M., Kaspi V. M., Qiao G., D'Amico N., 1992b, ApJ, 387, L37.
- Johnston S., Manchester R. N., Lyne A. G., Nicastro L., Spyromilio J., 1994, MNRAS, 268, 430
- Johnston S., Manchester R. N., Lyne A. G., D'Amico N., Bailes M., Gaensler B. M., Nicastro L., 1996, MNRAS, 279, 1026
- Kaspi V. M., Bailes M., Manchester R. N., Stappers B. W., Bell J. F., 1996, Nature, 381, 584
- Kaspi V. M., Tavani M., Nagase F. D., Hirayama M., Hoshino M., Aoki T., Kawai N., Arons J., 1995, ApJ, 452, 819
- King A., Cominsky L., 1994, ApJ, 435, 411
- Kochanek C. S., ApJ, 406, 638
- Kopal Z., 1978, Dynamics of Close Binary Systems, D. Reidel Publishing Company, Dordrecht, Holland
- Kumar P., Quataert E. J., 1997, ApJ, 479, L51
- Lai D., 1996, ApJ, 466, L35
- Lai D., 1998, ApJ, Submitted, astro-ph/9704132
- Lai D., Bildsten L., Kaspi V. M., 1995, ApJ, 452, 819
- Lyne A. G., 1996, Pulsars: Problems & Progress, ASP Conference Series, S. Johnston, M. A. Walker and M. Bailes, eds.
- Lyne A. G., Lorimer D. R., 1994, Nature, 369, 127
- Manchester R. N., Johnston S., Lyne A. G., D'Amico N., Bailes M., Nicastro L., 1995, ApJ, 445, L137
- Melatos A., Johnston S., Melrose D. B., 1995, MNRAS, 275, 381
- Nagase F., 1989, PASJ, 41, 1
- Porter J. M., 1996, MNRAS, 280, L31
- Schmidt-Kaler Th., 1982, in Scheifers K., Voight H. H., eds., Landolt Börnstein New Series, Vol. 2b. Springer-Verlag Berlin
- Schwarzschild M., 1958, Structure and evolution of stars, Princeton Univ. Press, Princeton
- Smarr L. L., Blandford, R. D., 1976, ApJ, 207, 574
- Slettebak A., Kuzma T. J. & Collins G. W., 1980, ApJ, 242, 171
- Standish E. M., 1982, A&A, 114, 297
- Taylor J. H., Weisberg J. M., 1989, ApJ, 345, 434
- Tavani M., Arons J., 1997, ApJ, 477, 439
- Waters L. B. F. M., 1986, A&A, 162, 121
- Wex N., 1998, MNRAS, In Press, (astro-ph/9706086)

Table 1. Parameters for the three timing solutions for PSR B1259–63, Model 1 (\ddot{P} , $\ddot{\dot{P}}$), Model 2A ($\dot{\omega}$, \dot{x}), and Model 2B ($\dot{\omega}$, \dot{x}). The data span is MJD 47909 – 50448. To estimate the parameter errors we compared all solutions for various combinations of integral numbers of phase turns at the two periastrons which give an rms residual not worse than 1.2 times the quoted rms residual. The error quoted in the table is the maximum difference between the values given in the table and the values obtained while changing the phase turns. Compared to the errors given by TEMPO and the errors obtained by the bootstrap method, the errors given here, in most cases, are more conservative.

	Model 1	Model 2A	Model 2B
Rms residual (μ s)	350	340	390
α (J2000)	13 ^h 02 ^m 47 ^s .65(1)	13 ^h 02 ^m 47 ^s .66(1)	13 ^h 02 ^m 47 ^s .65(1)
δ (J2000)	–63°50′08″.7(1)	–63°50′08″.7(1)	–63°50′08″.7(1)
P (ms)	47.7620537(1)	47.7620537(1)	47.7620537(1)
\dot{P} (10^{-15})	2.2785(2)	2.27709(1)	2.27720(1)
Epoch (MJD)	48053.440	48053.440	48053.440
DM (cm^{-3}pc)	146.78(5)	146.81(5)	146.85(5)
P_b (d)	1236.7238(1)	1236.7231(1)	1236.7244(1)
x (s)	1296.4(3)	1296.3(2)	1296.4(3)
ω (deg)	138.668(7)	138.667(6)	138.670(7)
e	0.86990(4)	0.86989(3)	0.86991(4)
T_0 (MJD)	48124.348(4)	48124.350(4)	48124.348(4)
\ddot{P} (10^{-26} s^{-1})	–5.2(8)	–0.884(9)	–0.788(1)
$\ddot{\dot{P}}$ (10^{-34} s^{-2})	+7(2)	—	—
$\ddot{\dot{P}}$ (10^{-42} s^{-3})	–5(2)	—	—
$\dot{\omega}$ (deg yr^{-1})	—	–0.000184(8)	–0.000396(9)
\dot{x} (10^{-10})	—	–0.15(3)	–2.40(4)
Epoch of Third periastron (UT)	1997/5/29 19 ^h	1997/5/29 19 ^h	1997/5/29 19 ^h